Feasibilityof Monitoring Large Wind Turbines Using Photogrammetry

Article *in* Energy · December 2010

DOI: 10.1016/j.energy.2010.09.008

CITATIONS
113

READS
326

4 authors, including:

Muammer Ozbek
Istanbul Bilgi University
24 PUBLICATIONS **363** CITATIONS

SEE PROFILE

Energy 35 (2010) 4802–4811

Contents lists available at ScienceDirect

Energy

journal homepage: www.elsevier.com/locate/energy

Feasibility of monitoring large wind turbines using photogrammetry

Muammer Ozbek [a,*], Daniel J. Rixen [a], Oliver Erne [b], Gunter Sanow [b]

[a] Delft University of Technology, Faculty of Mechanical Engineering, Mekelweg 2, 2628CD Delft, The Netherlands
[b] GOM mbH (Optical Measuring Techniques), Mittelweg 7-8, 38106 Braunschweig, Germany

ARTICLE INFO

Article history:
Received 3 May 2010
Received in revised form
31 August 2010
Accepted 5 September 2010

Keywords:
Wind turbine
Dynamic tests
Vibration measurements
Photogrammetry
Videogrammetry
Optical measurement techniques

ABSTRACT

Photogrammetry, which is a proven measurement technique based on determination of the 3D coordinates of the points on an object by using two or more images taken from different positions, is proposed to be a promising and cost efficient alternative for monitoring the dynamic behavior of wind turbines. The pros and cons of utilizing this measurement technique for several applications such as dynamic testing or health monitoring of large wind turbines are discussed by presenting the results of the infield tests performed on a 2.5 MW - 80 m diameter - wind turbine.

Within the scope of the work, the 3D dynamic response of the rotor is captured at 33 different locations simultaneously by using 4 CCD (charge coupled device) cameras while the turbine is rotating. Initial results show that the deformations on the turbine can be measured with an average accuracy of ±25 mm from a measurement distance of 220 m. Preliminary analyses of the measurements also show that some of the important turbine modes can be identified from photogrammetric measurement data.

1. Introduction

It is state of the art to use accelerometers and/or strain gauges placed inside the blade or tower for dynamic measurements performed on wind turbines [1–10]. However, these measurement systems are sensitive to lightning and electro-magnetic fields. Besides, some extra installations inside the blades such as placement of cables for power supply and data transfer are required for these applications. The signals from rotating sensors on the blades are transferred to stationary computer via slip rings or by radio/wireless transmission. For large commercial turbines the required installations and preparations (sensor calibration) might be very expensive and time consuming [11].

Moreover, the frequency range of the vibrations to be measured also limits the use of these sensors. Accelerometers cannot provide very accurate measurements for low frequency vibrations (0.3–1 Hz) that are expected to dominate the response of large wind turbines. Therefore only the higher frequency (greater than 1 Hz) vibrations can be captured accurately. The complicated nature of wind loads also makes the efficient use of these sensors on these specific structures very difficult. Since the deflections under the action of wind loading can be considered as the sum of a slowly changing static part and a rapidly changing dynamic part, identification of low frequency vibrations plays a crucial role in predicting the wind response of structures [12]. Several researchers reported that in wind response measurements, accelerometers should be used together with other systems such as GPS (Global Positioning System) which are able to detect these low frequency motions accurately [13–15]. However, it is also not practical to place the GPS sensors in the blade structure.

Fiber optic strain gauges are proposed to be a promising alternative to accelerometers and conventional strain gauges since optical sensors are not prone to electro-magnetic fields or lightning. However, it is reported that some additional feasibility tests are still needed to ensure the effective and cost efficient use of this measurement system. The factors affecting the performance of the fiber optic sensors such as sensitivity to humidity and temperature variations and the required error compensation methods should also be investigated further [16,17].

This work aims at investigating the feasibility of applying photogrammetry to large wind turbines and the accuracy that one can expect with current state-of-the-art software and hardware. The final goal is to use the measurements for model verification and health monitoring of wind turbines. Hence, as a following study after the estimation of the measurement accuracy, the applicability of Operational Modal Analysis on the measurements to identify the modal behavior of wind turbines will be discussed as the next research step.

2. Photogrammetric measurement techniques

Photogrammetry is a measurement technique where 3D coordinates or displacements of an object can be obtained by using the

* Corresponding author. Tel.: +31 15 2789514; fax: +31 15 2782150.
E-mail address: m.ozbek@tudelft.nl (M. Ozbek).

0360-5442/$ – see front matter © 2010 Elsevier Ltd. All rights reserved.
doi:10.1016/j.energy.2010.09.008

2D images taken from different locations and orientations. Although each picture provides 2D information only, very accurate 3D information related to the coordinates and/or displacements of the object can be obtained by simultaneous processing of these images as displayed in Fig. 1.

Several applications of photogrammetric measurements are currently in use and proven to provide very accurate measurements for a wide variety of disciplines. The method is sometimes called "videogrammetry" (which implies that sequences of the pictures are used to monitor the dynamic response of an object) or "stereo-photogrammetry" (indicating that two or more cameras are employed simultaneously). Despite these minor differences, all the methods are based on similar mathematical relationships established between the 3D position of an object and its 2D representations [18].

Although photogrammetry is widely used in measuring the coordinates and displacements of the objects, its use is limited to small measurement volumes and the measurements are usually performed in laboratories or similar controllable environments. Within this small measurement volume it can be efficiently used for different purposes such as;

- 3D shape determination, modeling and reverse engineering [19–21]
- Static or dynamic deformation measurements [22–30]
- Modal analysis and system identification [31–36].

Photogrammetry can also be used within large volumes but these measurements are typically static. 3D modeling and reverse engineering are usually the only application fields. However, efficient use of photogrammetry in large measurement volumes for dynamic measurements is still unknown. There are some important issues to be considered before utilizing this technique for monitoring of large structures such as wind turbines which have very specific characteristics and challenging operating conditions.

The size of the object to be tracked is usually restricted due to the problems such as insufficient illumination, difficulties in calibration, or low resolution of the cameras. If the target to be tracked (for instance the tip of the blade) experiences large displacements and rotations throughout the measurement volume, this can result in significant changes in reflection angles and the orientation of the targets during the measurements. Besides, these targets should also be illuminated sufficiently during the entire measurement, and the only possible solution is to illuminate the whole measurement volume.

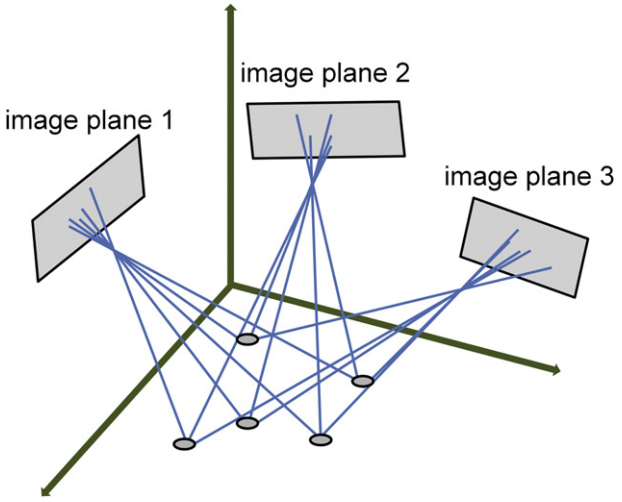

Fig. 1. Simultaneous process of 2D images taken from different locations.

For rapidly moving objects, the shutter time (i.e. the period during which the image is created by the light entering through the shutter) should be small enough to limit blurring caused by the motion of the object during the formation of the image. However, if the shutter time is very small, proper illumination becomes more important and a stronger light intensity is needed to provide sufficient contrast. In addition to these problems, since the number of pixels (resolution) of the utilized camera systems is limited, the pixel per area is significantly reduced if the area to be viewed is very large.

Corten and Sabel [11,37] were the first in applying this measurement method to a wind turbine. They performed several vibration measurements on a 2 bladed wind turbine (10 m diameter) while the turbine was in operation. For this purpose, they placed several markers both on the blades and on the tower. In order to increase the measurement accuracy they located the camera systems on tripods whose heights were approximately one third of the height of the tower. Such an approach would certainly improve the accuracy of the photogrammetric measurements but at the same time makes the applicability of the method to larger turbines more difficult. Based on the results of the consistency checks, the authors reported that the measurement error was directly related to the size of the observed object or field and in the range of 0.043% (or 1/2500) of field of view. Corten and Sabel also aimed at comparing the measured 3D coordinates with the strain measurements taken by strain gauges installed in the blades but they could only compare the two data sets for a qualitative confirmation of the method. Quantitative comparisons showed large differences. The authors concluded that both systems in fact measure different physical quantities, and that some motions such as bending of the rotor axis, small tilt and yaw motion of the nacelle and teeter cannot be detected by strain gauges. Even detectable motions might not have a linear relationship with the strains measured locally. However, the authors also reported that photogrammetry would be a very promising method to monitor wind turbine dynamics if the hardware and software technology progressed.

The photogrammetric measurements presented in this article were performed similarly to Corten and Sabel [11,37] in terms of using reflective round markers and post-processing the image. In the present work however, state-of-the-art software and hardware were used, all the measurement systems were located on the ground and a very large turbine was measured in operation.

3. Measurement setup

3.1. The test turbine

Our tests were conducted on a pitch controlled, variable speed Nordex N80 wind turbine with a rated power of 2.5 MW. The turbine has a rotor diameter and tower height of 80 m and can be considered as one of the largest wind turbines that are commercially available at the time the tests were conducted. Detailed information about the technical properties of the wind turbine can be obtained through the website of the manufacturer [38].

The measurements were performed by GOM mbH [39] (GOM Optical Measuring Techniques) at the ECN (Energy Research Center of the Netherlands) wind turbine test site located in Wieringermeer, the Netherlands. More detailed information about the facilities of the test site can be found through the related website [40].

3.2. Camera layout and marker placement

Fig. 2 shows the measurement setup and the layout of the camera-flash systems. A modified GOM PONTOS system consisting

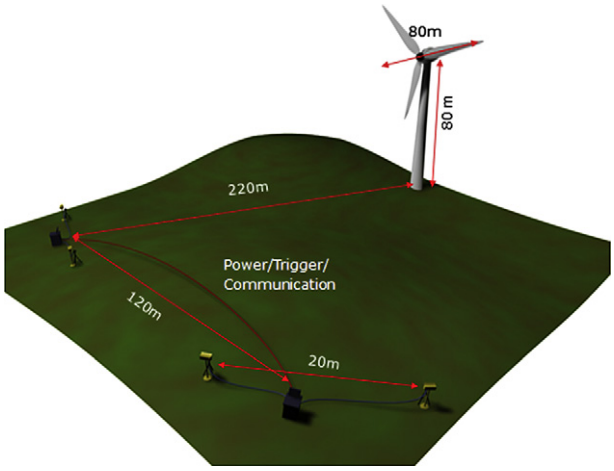

Fig. 2. The Measurement setup and camera locations (provided by GOM mBH [39]).

of four CCD cameras was used to monitor the dynamic behavior of the turbine in operation. The whole turbine structure was captured in all the pictures taken which resulted in a very large area (120 m high - 80 m wide) to be viewed by each camera continuously during the entire measurement period. The distance between the camera-flash light systems and the turbine was 220 m.

The cameras and the high intensity LED (light emitting diode) based flashes were synchronized by a central PC. This central PC controlled all the communication between the data acquisition system and the cameras, and also the triggering signals and power transferred to the flashes. The sampling frequency of the measurements was 28 Hz which can be considered sufficient compared to the frequency range (0.3–5 Hz) of the vibrations expected to be observed.

Photogrammetry requires some markers to be placed on the object to be tracked. The camera systems follow the motion of these markers from different orientations and construct the 3D deformation vectors. These markers are made up of retro-reflective materials (1000 times more reflective than the background material) to increase the reflectivity of the target and to provide a better visibility. In our testing, a total of 55 markers (11 markers on each blade and 22 markers on the tower) were placed on the turbine. Since they are in the form of very thin stickers (round shaped - 400 mm diameter), they are not expected to affect the structural or aerodynamic properties of the blade. Fig. 3a and b shows the placement of the markers on the turbine.

It should be noted that it only took 2 professional people 6 h to place 55 markers on the turbine. Considering the fact that each marker acts as an independent sensor, it can be concluded that it is almost impossible to reach such a high sensor installation speed by using conventional sensor technologies (accelerometers, piezo-electric or fiber optic strain gauges). The final distribution of the markers on the turbine can be seen in Fig. 4a–b. Although the pictures shown in Figs. 3 and 4 were captured by a handheld digital camera using its flash light only, the markers can be seen easily. The displacement data obtained by using the tower markers are not presented or used in this article since tower measurements were interrupted each time a blade passed in front of it.

3.3. Illumination requirements

Proper illumination plays a crucial role in obtaining high quality images. Initial computer simulations and feasibility tests showed that the use of conventional flash-light systems would require a large amount of power for the flashes. In order to prevent the technical problems that can be encountered due to this high power requirement, a different high intensity LED based flash system was used for the measurements. For this LED illumination system a power supply of 2 kW (provided by a small size commercial generator) was sufficient to illuminate the turbine throughout the measurements.

However, the use of this new flash system during daytime is limited. In photogrammetry, the contrast between the marker and the background material is very important. If a weak flash is used during daytime, the difference between the reflection of the flash light from the marker and the reflection of the sun light from the background material is not so high. The advantage of the retro-reflective material is that it directly reflects the light beam back to its source and it is 1000 times more reflective than the blade material but despite all these advantages sun light will always be more dominant. Therefore to get a high contrast without using a powerful flash light the experiments were conducted during night time.

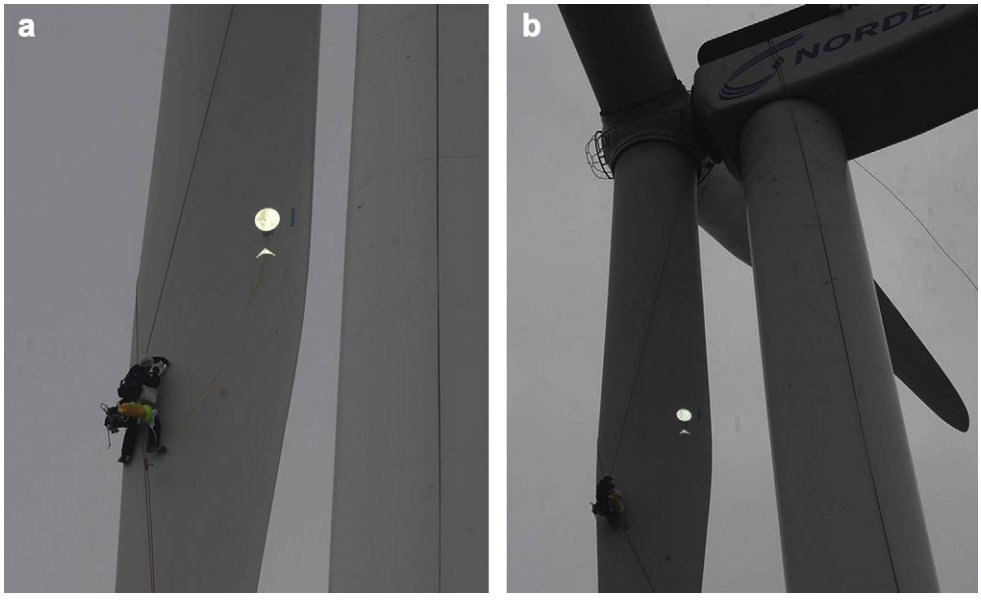

Fig. 3. a–b: Installation of markers on the wind turbine.

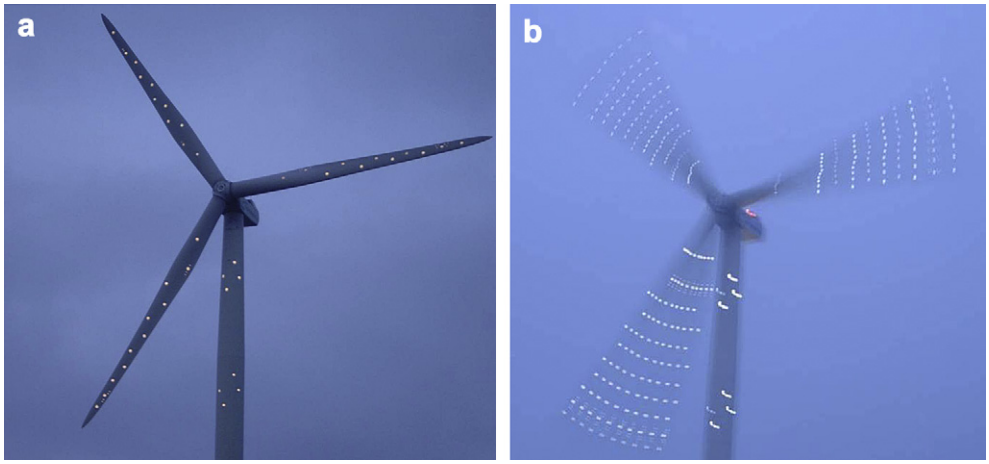

Fig. 4. a–b: The Layout of markers on the turbine.

As the size of the object to be tracked increases, illumination and the required power become a more critical problem. Several researches [21] reported that they had to perform the photogrammetric measurements in a dark laboratory environment because the sufficient contrast levels could only be reached when the ambient lighting was off and the LED based flashes were used as the only light source in the experiment.

3.4. Camera calibration

Calibration of the cameras is one of the most important factors that directly affect the accuracy obtained and can be investigated in 2 groups namely intrinsic and extrinsic calibration. The intrinsic calibration is required to determine the geometrical and optical characteristics of the cameras whereas; the extrinsic calibration parameters describe the camera positions and orientations with respect to a predefined global coordinate system.

Conventional camera calibration techniques can be roughly classified into two categories: photogrammetric calibration and self-calibration. For photogrammetric calibration, a calibration object having similar dimensions with the measured structure is used. This calibration object can be either a 3D object or a 2D planar pattern with precisely known geometry and dimensions. Although this technique is widely used for the measurements taken in the laboratory environment, for the tests performed on large structures the use of these calibration tools is highly unpractical.

On the other hand, self-calibration (bundle adjustment method) is performed using a set of highly convergent overlapping images only. Any photogrammetric network comprising two or more camera stations and sufficient number of control points (common to each image) constitutes an over-determined nonlinear observation equation system, the parameters for which can be obtained via a least-squares estimation process [28]. This method also enables both extrinsic and intrinsic calibration parameters to be determined simultaneously.

In this study, the camera calibration was performed by using the markers distributed throughout the turbine structure and the mentioned least square based calibration algorithm. A small 2D planar pattern was also utilized to provide supplementary information related to the internal camera optical parameters.

4. Acquiring vibration data and post-processing

Since the turbine was not kept at a fixed yawing angle during the measurements, the relative angle between the normal of the rotation plane and the 4 camera axes changed during the measurements. In order to prevent possible sources of error, rotation plane and the corresponding axes attached to this plane were continuously updated throughout the measurements. The deformations shown below were defined with respect to this continuously updated rotation plane and coordinate axes.

The first step in calculating the rotation plane is the determination of center of rotation. Since the markers on the rotor are moving on a circular path, this can easily be done by observing the path travelled by a marker and fitting a circle to it by using a least square based algorithm. This operation is performed for several markers. The resultant center coordinates can be slightly different depending on the marker chosen. Therefore the average of the coordinates are calculated and used to minimize the error.

Following the calculation of rotation center and plane, a rigid body correction (also called as de-rotation) is applied to the actual deformation vectors measured. A marker selected to be tracked experiences very large displacements during a complete cycle of the blade. Hence, the displacement component coming from rigid body motion of the rotor is subtracted from the measured real displacement of each marker to provide a better visualization and interpretation of the data. Therefore, although the results displayed below include rotational effects they can be evaluated as if they were measured on a stationary (parked) turbine vibrating under the action of wind loads.

A typical displacement time history measured in flapwise direction for the tip markers of 3 blades can be seen in Fig. 5. It should be noted that these displacements are calculated with respect to the initial coordinates of the markers described by the first picture taken during rotation. Since the blades are already deformed under the action of wind loads at this instant, the first image used as the reference is not expected to represent the exact undeformed shape of the rotor. However, the selection of initial coordinates does not have an effect on the amplitudes of the calculated relative displacements or the accuracy of the measurements. In Fig. 5 the horizontal axis represents the number of rotation cycles in the recorded data. The maximum (peak to peak) amplitudes of the relative displacements measured during 5 different measurements are displayed in Table 1. It can be seen that the tip of the blade can experience a relative displacement up to 102.4 cm during rotation.

5. Estimation of the measurement accuracy

In photogrammetry, the measurement accuracy is usually described either in terms of pixel or the ratio of the absolute measurement error to the field of view. The accuracy is mainly related to

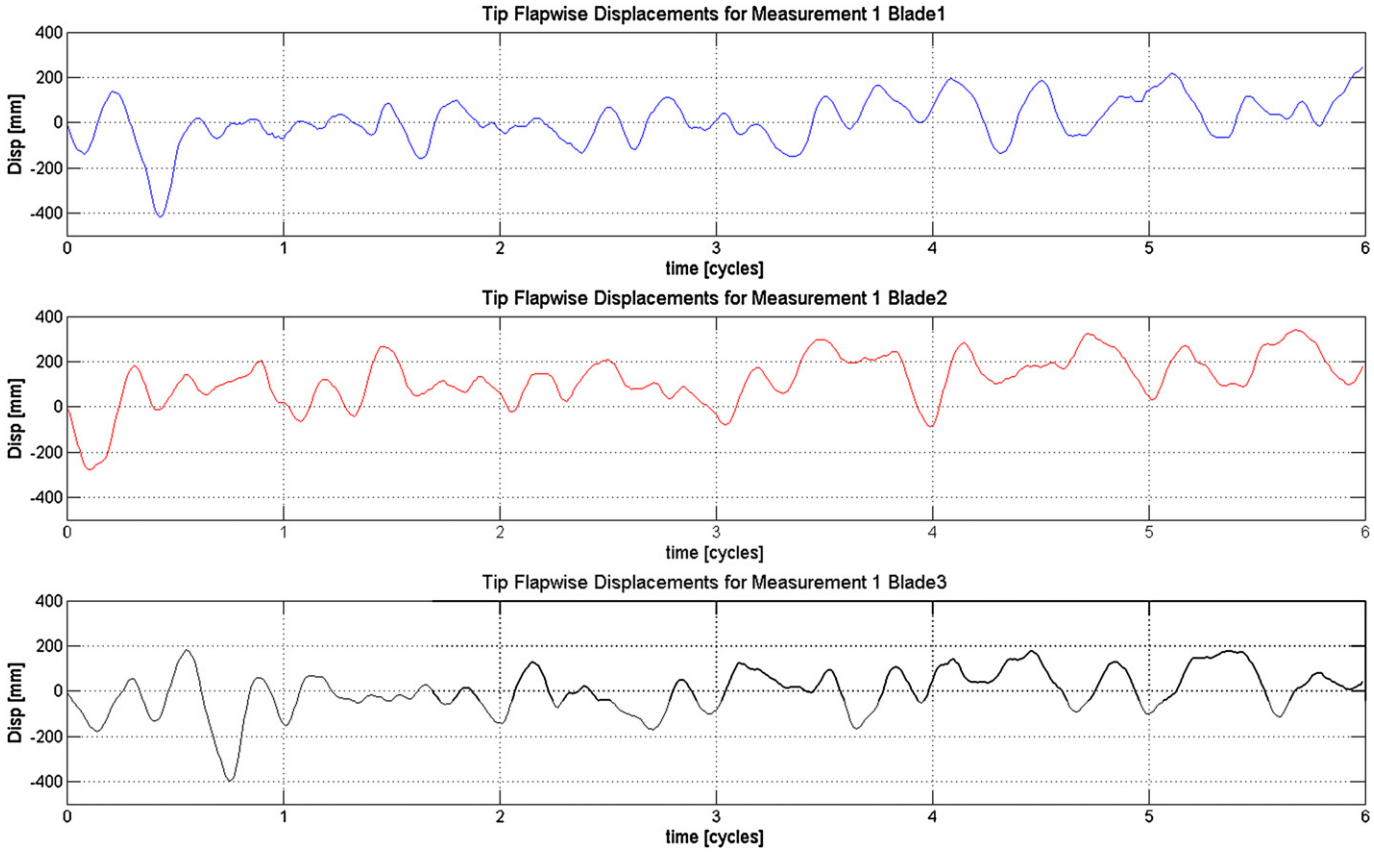

Fig. 5. Time normalized tip flapwise displacements recorded during measurement 1.

the type and resolution of the cameras, illumination intensity, the size and visibility of the targets, and camera calibration.

Very high accuracies such as 1/50,000 (1 part in 50,000) of the observed field of view can be reached in controllable laboratory environments by using 3D calibration tools, 3D control targets and powerful illumination systems, but these ideal conditions are generally not met for infield tests performed on large wind turbines.

Several researchers performing indoor photogrammetric measurements similar to those described in this work, report average accuracies varying between 1/8000 and 1/15,000 [28–31]. An extensive research program has been recently conducted by NASA to investigate the feasibility of using photogrammetry to measure the dynamic behavior of ultra light weight membrane-type space structures. Results indicate that the coordinate measurement errors calculated for *X*, *Y* and *Z* axes may differ significantly depending on the locations and the orientations of the cameras and the direction of the observed motion [21,26]. In-plane coordinates and displacements can generally be measured with accuracies changing between 1/28,000 and 1/14,000 of field of view. However, the errors calculated for out-of-plane direction (depth) are much larger and in the range of 1/5000. The researchers also reported that these values represent random measurement errors and can only be used for the overall measurement accuracy if systematic or gross errors are negligible [26]. It should be noted that these accuracies are computed for test objects having dimensions varying between 5 and 15 m and test setups in which no major systematic measurement errors are expected. However, wind turbines have very distinct features (large dimensions, components rotating at very high speeds and continuously changing reflection angles) which make photogrammetric measurements much more challenging.

Table 1
The flapwise displacements (peak to peak) calculated for tip marker through measurement 1–5.

Relative Tip Disp. (mm)	M1	M2	M3	M4	M5
Blade 1 - tip marker	659	605	670	1024	1005
Blade 2 - tip marker	617	594	703	895	898
Blade 3 - tip marker	576	695	699	1007	961

A common method to determine the measurement accuracy is to compare the 3D target coordinates reconstructed from photogrammetry with those measured by more accurate surveying systems such as theodolites, “total stations” (used in monitoring of civil engineering structures) or laser measurement devices. However, these systems measure the marker coordinates not simultaneously but sequentially. Since the markers on a wind turbine in the field are never fully at standstill, such measurements would not be suitable to validate the calibration parameters and to determine the measurement accuracy. Therefore, all the critical pre or post-processing operations and the corresponding error estimation analyses have been done by using the measurements themselves i.e. by verifying the consistency of the data recorded.

In our tests, the error was estimated by checking whether or not the distance between target points remains constant throughout the measurement. In particular, we will use the fact that the distance between the calculated center of rotation and a marker should barely change in time and can thus be used to estimate the accuracy of the measurements. Negligible length changes are expected in the blades due to centrifugal or gravity forces acting on the rotor and the out-of-plane deformation is small compared to the distance between selected points. If any difference (called as elongation or contraction in this text) is observed, it can mainly be

attributed to the inaccurate measurement of the marker coordinates and therefore, can be used to estimate the accuracy.

The measurement errors revealed by the change of distance between markers and the center of rotation are expected to be mainly caused by calibration problems, reflection quality changing during the rotation and some other physical factors affecting the visibility of the markers. Depending on these factors, the measurement errors can be classified in two groups, namely *random* and *systematic* errors.

Fig. 6 displays the labeling of the markers used to compute elongations and thereby estimate the error. It can be seen from this figure that the markers are placed on surfaces having different curvatures, which directly affects the intensity of the reflected light and the shape seen by the cameras. The markers close to the tip were placed on a relatively flat surface whereas the ones close to the hub are placed on a more curved surface. It should be noted that the marker located between 1 and 2 was dysfunctional and not used in the analyses.

The light reflected by the marker and their recorded shape will also vary during the rotation of the rotor of the turbine, inevitably affecting the quality of the measurements. Fig. 7 displays how the horizontal reflection and camera view angles change during a complete cycle of rotation. It should be noted that the effective view or reflection angle is a combination of horizontal and vertical angles and cannot be fully represented in a 2D plot. As can be seen from Fig. 7 the horizontal reflection angles can vary between 0 and 30° for the tip marker. Similarly, the vertical reflection angles can change between 15 and 35°.

Fig. 8 and Fig. 9 display the change of the distance (also called as elongation) between the center of rotation and markers 10 and 1 respectively. It should be noted that the original data blocks include 6 complete cycles of rotation. In order to see the repeating pattern of the change, the analyzed record was divided into 6 parts and these cycles were superposed in the plots of Figs. 8 and 9, as a function of the azimuth angle (zero when the blade is at the top). For Fig. 8 the legend G1 B1 M10 C1 stands for (G1) Measurement 1 − (B1) Blade 1 −(M10) Marker 10 − (C1) Cycle1. These figures show the elongation values obtained by applying a low-pass filter with a cut-off frequency of 5 P (P being the rotation frequency of the rotor) on the raw data. The high frequency component, which is attributed to the random measurement error, has only a minor contribution (±5 mm) and will be eliminated by the applied low-pass filter.

In Figs. 8 and 9 the polar plots on the right show where the maximum elongation points are reached for markers 5 to 10. It can easily be noticed from the figures that the elongation is highly periodic and azimuth-angle dependent, which implies that it is mainly caused by repeating systematic errors. In order to check the reliability of the elongation information, these analyses were conducted for different measurements and for the entire set of 33 markers placed on the rotor. The comparisons showed that, although the 3D displacements experienced by the markers may differ depending on the test number, the graphs of the calculated elongations were almost identical for the markers that are placed on similar locations on the blade, which strongly reinforces the fact that there is a systematic measurement error whose amplitude is determined by the location of the marker only.

Fig. 6. The locations and corresponding labeling of the markers used in error estimation.

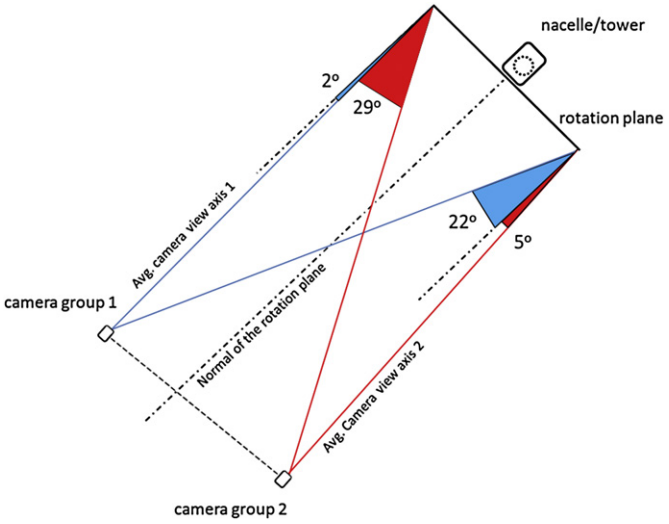

Fig. 7. The change of horizontal reflection angles (for tip marker) during rotation.

Repeating systematic errors can be caused by different physical factors, which have different periodic effects on the system. A variation in the reflection quality is expected to appear once per cycle and will thus cause a dominant 1P component, where P denotes the rotational frequency of the rotor. On the other hand, calibration problems (either internal or external), or miscalculation of the rotational plane can cause a harmonic elongation twice a cycle and have a dominant 2P component. Similarly, a measurement error of 2P is likely to occur when the tracked marker passes through the regions where the view and reflection angles approach to the limit values. During the rotation, the markers move on a circular path, which should be fully captured in each one of the 2D images analyzed. For the outermost markers the horizontal and vertical view angles approach to critical values twice a cycle.

The instantaneous location of the traced marker in the 2D image i.e. its distance to the edges of the 2D picture can be related to the amplitude of the elongation measured at that location. As can be seen in Fig. 8, the amplitudes of the elongations calculated at around 90 and 270 degrees of azimuth angles are not the same. Normally, the same amount of error would be expected for these locations. Since the center of rotation does not exactly coincide with the center of the image, the markers are closer to the edge of the 2D image around 270° azimuth than they are at around 90° azimuth. The rotor which is eccentrically located in the 2D image causes the systematic measurement errors to differ at those locations.

6. Order analysis of the elongation error

The frequency domain analysis of the elongation data provides important information to be used in determining the source of the error. Fig. 10 aims at showing the important frequencies identified in the corresponding length changes. The frequencies, normalized with respect to the rotational frequency, are displayed along the *X*-axis. The *Y*-axis represents the marker number. The numbering of the markers was depicted in Fig. 6. The *Z*-axis represents the amplitude of the Fourier transform. As can be seen from the figure the change of the distance calculated for marker 10 has a strong 2P and a relatively weaker 1P component whereas the one calculated for marker 1 has a very dominant 1P and a much weaker 2P component. 1P and 2P components always exist in the Fourier transforms of the elongation data but their relative amplitudes differ depending on the location of the marker.

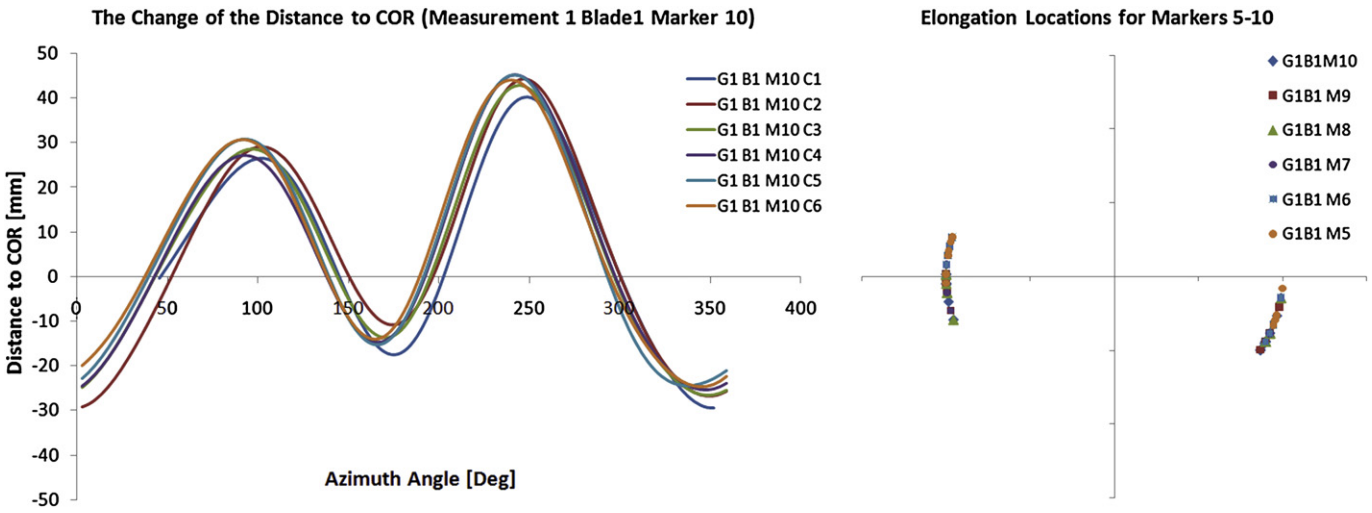

Fig. 8. Elongation between marker 10 and center of rotation. Polar locations of maximum elongation for M5-M10.

Markers 1 and 2 are placed on curved surfaces close to the root of the blade. The measurement errors calculated for these markers are expected to be mainly related to the reflection quality and marker orientation varying during the rotation. Although 1P component of the error can be seen in all the 10 series its contribution in the overall error is dominant for Markers 1 and 2 only. As the distance from the center of rotation increases the contribution of 2P component gradually becomes more important, probably because those markers are closer to the boundaries of the field of view where calibration errors and artifacts due to projection on the plane of rotation become more dominant.

Let us observe in Fig. 10 that the contribution of order of 3P (as well as all higher orders) is significantly lower than the components of order 1P and 2P, and they will not be further discussed.

7. The possibility of correcting the systematic measurement errors

From the discussion in the previous section, it is clear that the causes of systematic errors can be traced back to geometry and optical effects varying along the circular path of the markers in the field of view of the cameras. Hence one could be tempted to use this knowledge to correct the measurements for those errors, such that the only remaining errors would be the random errors (arising from unavoidable pixel quantization and fitting errors).

Three different approaches can be potentially used for performing such a correction in future research.

a. Properly calibrating the measurement setup by identifying the systematic error for all locations of the field of view. This would require either a very detailed theoretical analysis of optical errors and marker orientation effects, or a reference measurement using lasers for instance. Such an approach seems however difficult and unpractical.

b. Estimating the error using the computation of elongations as described in the previous two sections, one could try to reconstruct the error in the 3D coordinates of the markers. Assuming for instance that the position of the center of rotation is estimated without error, and having good knowledge on the statistical distribution and correlation of the coordinate error at the different locations of the field of view, one could estimate the most likely position of the marker.

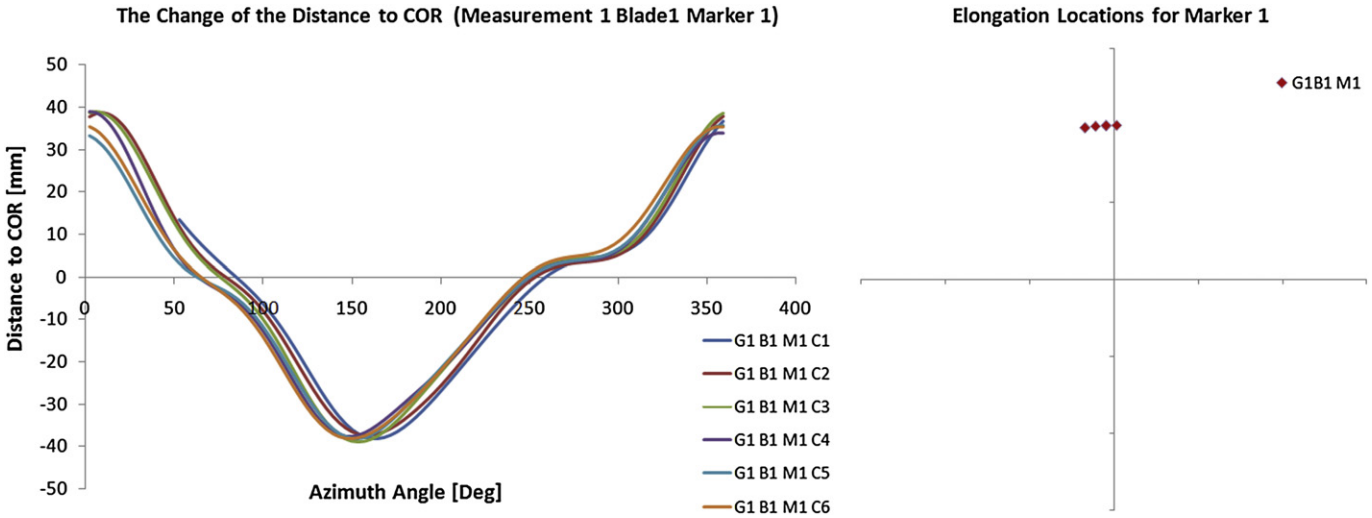

Fig. 9. Elongation between marker 1 and center of rotation. Polar locations of maximum elongation locations for M1.

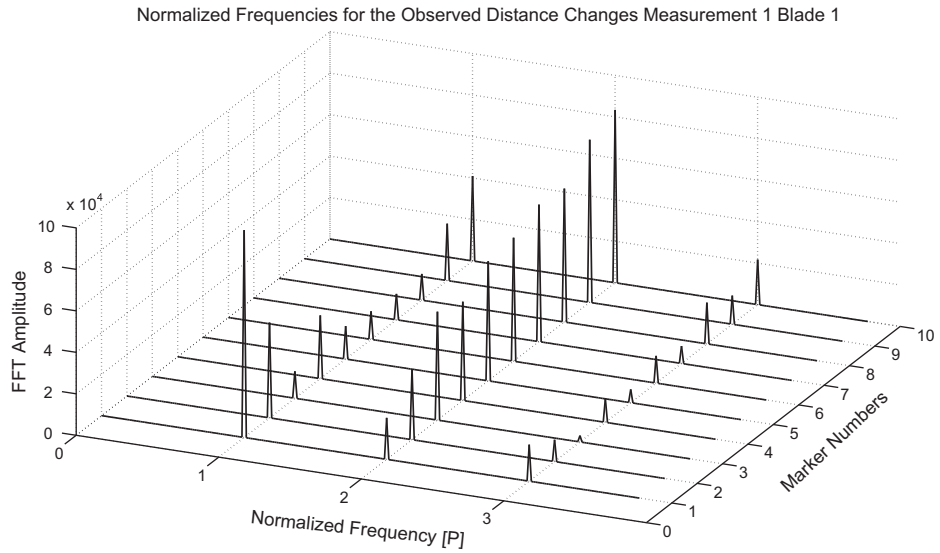

Fig. 10. The frequency distribution of the observed distance changes (Measurement 1, Blade 1).

c. One could also use a priori knowledge about the expected deformation of the blades. As an example, consider the components of order 1P of the systematic error in Fig. 10. Such a contribution to the deformation of the blade in the low frequency range is not expected. Hence projecting the measurements on a small set of expected deformation modes (obtained for instance from simple beam theory) could lead to a procedure to filter out part of the measurement error. Note however that the 2P contribution to the systematic error will probably not be removed by such a spatial filtering approach since, as can be seen in Fig. 10, the 2P components exhibit a spatial distribution along the blade that is similar to the expected deformation. This is due to the very origin of the 2P as explained in the previous section. Hence such an approach would mainly smooth out the errors observed on markers 1 and 2.

8. Frequency domain investigation of measured vibration data

Fig. 11 and Fig. 12 show typical examples of PSD (Power Spectral Density) graphs of edgewise and flapwise vibrations measured by photogrammetry. It should be noted that all the frequencies displayed below are normalized with respect to the rotational frequency. In order to protect the manufacturer's interests, the real frequencies are not given explicitly in this article. Figs. 11 and 12 are presented to provide a 3D frequency distribution which also includes the information related to the measurement location. The *X*-axis represents the normalized frequencies identified from the analyzed data; the *Y*-axis corresponds to the marker number (defined in Fig. 6) and the *Z*-axis represents the computed PSD amplitude. The 1P and 2P components, and first edgewise mode can be recognized from Fig. 11.

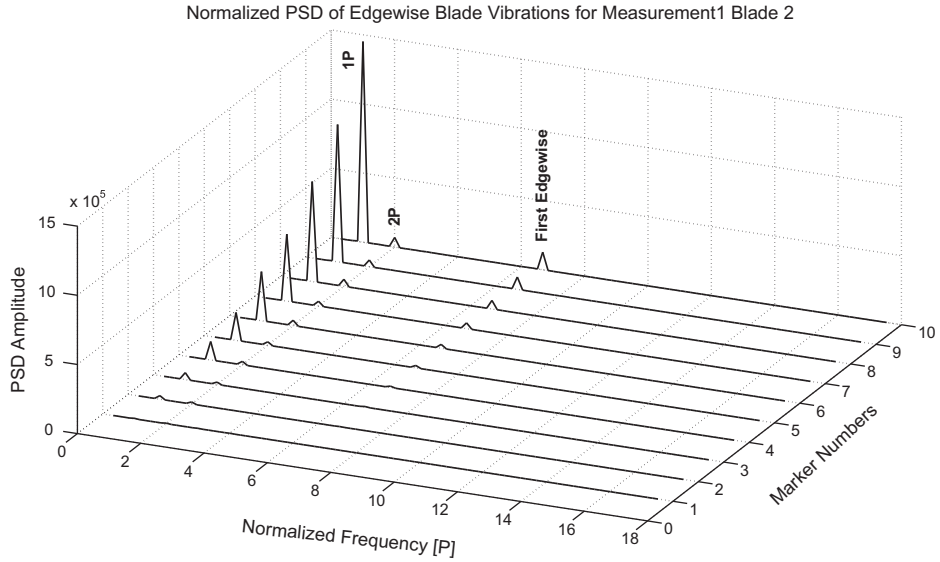

Fig. 11. Normalized PSD of edgewise blade vibration for measurement 1 Blade 2.

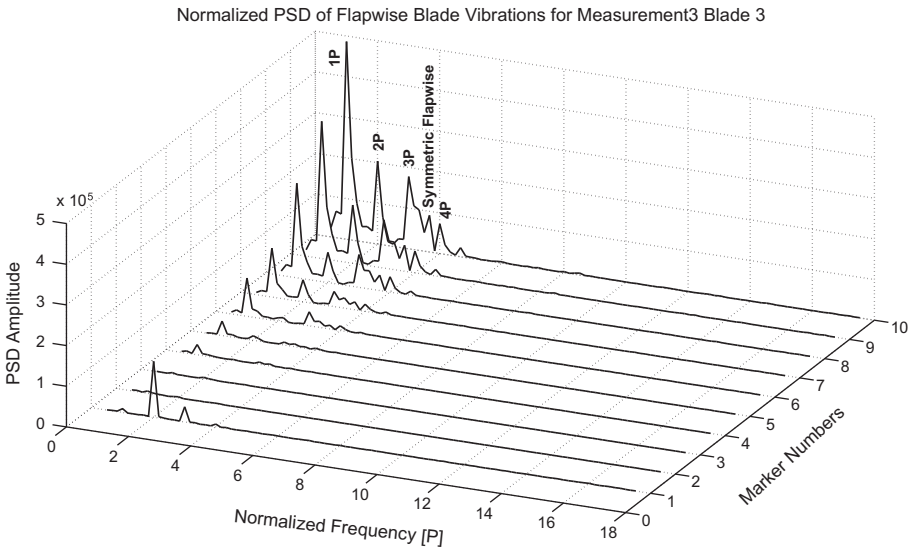

Fig. 12. Normalized PSD of flapwise blade vibration for Measurement 3 Blade 3.

As can be seen from Fig. 12, flapwise vibration data enables more frequencies to be identified. The integer multiples of rotation frequency up to 4P can be detected from the corresponding PSD graph. The contribution of these P components in the overall motion is consistent with those reported by several researchers [41,42]. Besides these P components, first flapwise mode can also be seen in Fig. 12.

Since the response is mainly dominated by the integer multiples of rotational frequency (P components) the other turbine modes which have relatively weaker participations in the overall response and which can also exhibit significant damping cannot be identified easily from PSD plots only. However, several system identification methods enable weaker frequencies to be detected. A more detailed investigation [43] of the measured turbine response carried out by utilizing these identification methods showed that the second edgewise, second and third flapwise modes of the blades can also be identified. However, further analyses and measurements are needed for validation of observability of these high frequency modes from photogrammetric measurements.

9. Conclusion

Based on the results of the analyses reported in this paper, it can be concluded that the random component of the coordinate measurement error is in the range of ±5 mm or 1/16,000 of field of view. This amount is consistent with the random measurement errors reported in literature. If compared to the amplitudes of the deformations (summarized in Table 1) that are expected, this accuracy can be considered to be high and even be improved further by using higher resolution cameras.

Initial results show that the deformations on the turbine can be measured with an average accuracy of ±25 mm from a measurement distance of 220 m, which is the overall error including both the systematic and the random errors. The maximum value of the systematic error (2P component) was found to be of the order of ±30 mm in our calculations, the maximum being found for the outermost markers. Since the random error component is usually in the range of ±5 mm, independent of the marker location, the maximum overall error could reach 35 mm for the tip marker. However, using more sophisticated camera calibration, data processing and comparison techniques can reduce the systematic error further. These ideas are at the center of current research. Although 1P component of the error can even have higher amplitudes, this can easily be eliminated by spatial filtering, therefore it is ignored.

Even though the measurement error was found to be of the order of 10 percent of the recorded deformations (displayed in Fig. 5 and summarized in Table 1), the data obtained from photogrammetry appeared to be suitable to identify the 1P - 4P modes, as well as some of the lower eigenmodes and eigenfrequencies of the blades in operation. First edgewise and first flapwise modes can easily be identified from Figs. 11 and 12, respectively.

Some other turbine modes having relatively weaker participations can also be identified by using more sophisticated identification algorithms which were not explained in detail in this article. A more comprehensive discussion about the identification of these modes can be found in [43]. The accuracy of the identified modal properties can be increased by reducing the measurement errors (as explained above), performing longer measurements and improving the operational modal analysis methods as pointed out in [43].

Developments over the last decade have resulted in higher resolution and more sensitive cameras, and in efficient software for photogrammetry, so that we believe that photogrammetry can be a versatile and cost-effective technique for health monitoring and dynamic validation of wind turbines.

The markers which are used as displacement sensors can easily be placed on an existing turbine. No extra cable installations for data transfer and power supply are required inside the turbine. Therefore, compared to the conventional sensors (accelerometers, piezoelectric or fiber optic strain gauges), marker installations are very cost efficient and can be completed within very short periods of time. Retroreflective paints applied on the turbine components during the manufacturing stage in the factory can substitute these markers which may result in a further decrease in the installation costs.

A photogrammetric measurement system which consists of several CCD cameras, flashes and a central PC can be re-used for monitoring several turbines. If continuous monitoring is not required, all the turbines in a wind farm can be observed by using a single system. The measured data can be stored and used to build a condition monitoring archive. Since all the measurement systems are located on the ground, a possible technical problem can be detected and solved easily.

Wind turbines have very specific characteristics and challenging operating conditions. Although the photogrammetric measurement systems (including both the hardware and image processing

software), calibration methods and utilized operational modal analysis techniques were not specifically designed and optimized to be used for monitoring large wind turbines, the accuracy reached in this feasibility study is very promising. It is believed that this accuracy can easily be increased further by utilizing more specialized hardware and data processing methods.

Acknowledgements

This research project was partly funded by the We@Sea research program, financed by the Dutch Ministry of Economical Affairs.

The authors would like to thank ECN (Energy Research Center of the Netherlands) for providing the tests turbine and other technical equipment.

The authors also acknowledge the extensive contribution of Pieter Schuer (GOM mbH), Wim Cuypers (GOM mbH), Theo W. Verbruggen (ECN) and Hans J. P. Verhoef (ECN) in organizing and performing the field tests.

References

[1] Carne TG, Nord AR. Modal testing of a rotating wind turbine. Sandia National Laboratories; 1983. SAND82–0631.
[2] Malcolm DJ. Dynamic response of a Darrieus rotor wind turbine subject to turbulent flow. Engineering Structures 1988;10:125–34.
[3] James GH, Carne TG, Lauffer JP. The natural excitation technique (NExT) for modal parameter extraction from operating wind turbines. Sandia National Laboratories; 1993. SAND92–1666.
[4] Malcolm DJ. Structural response of 34-m Darrieus rotor to turbulent winds. Journal of Aerospace Engineering 1993;6(1):55–75.
[5] James GH, Carne TG, Veers PS. Damping measurements using operational data. ASME Journal of Solar Energy Engineering 1996;118:190–3.
[6] Wright AD, Kelley ND, Osgood RM. Validation of a model for a two-bladed flexible rotor system: progress to date. In: 37th AIAA aerospace sciences meeting. Reno, Nevada; 1999. AIAA-1999–0060.
[7] Thomsen K, Petersen JT, Nim E, Øye S, Petersen B. A method for determination of damping for edgewise blade vibrations. Wind Energy 2000;3:233–46.
[8] Molenaar DP. Experimental modal analysis of a 750 kW wind turbine for structural model validation. In: 41st aerospace sciences meeting and exhibit. Reno, Nevada; 2003. AIAA-2003-1047.
[9] Hansen MH, Thomsen K, Fuglsang P. Two methods for estimating aeroelastic damping of operational wind turbine modes from experiments. Wind Energy 2006;9:179–91.
[10] Kong C, Bang J, Sugiyama Y. Structural investigation of composite wind turbine blade considering various load cases and fatigue life. Energy 2005;30:2101–14.
[11] Corten GP, Sabel JC. Optical motion analysis of wind turbines. SV Research Group. Delft University of Technology, ISBN 90-75638-01-9; 1995.
[12] Tamura Y, Matsui M, Pagnini LC, Ishibashi R, Yoshida A. Measurement of wind-induced response of buildings using RTK-GPS. Journal of Wind Engineering and Industrial Aerodynamics 2002;90:1783–93.
[13] Nakamura S. GPS measurement of wind-induced suspension bridge girder displacements. ASCE Journal of Structural Engineering 2000;126(12):1413–9.
[14] Breuer P, Chmielewski T, Gorski P, Konopka E. Application of GPS technology to measurements of displacements of high-rise structures due to weak winds. Journal of Wind Engineering and Industrial Aerodynamics 2002;90(3):223–30.
[15] Nickitopoulou A, Protopsalti K, Stiros S. Monitoring dynamic and quasi-static deformations of large flexible engineering structures with GPS: accuracy, limitations and promises. Engineering Structures 2006;28:1471–82.
[16] Rademakers LWMM, Verbruggen TW, van der Werff PA, Korterink H, Richon D, Rey P, et al. Fiber optic blade monitoring. In: European Wind Energy Conference. London; 2004.
[17] Schroeder K, Ecke W, Apitz J, Lembke E, Lenschow G. A fiber Bragg grating sensor system monitors operational load in a wind turbine rotor blade. Measurement Science and Technology 2006;17:1167–72.
[18] Mikhail EM, Bethel JS, McGlone JC. Introduction to modern photogrammetry. New York: Wiley; 2001.
[19] Pauwels S, Debille J, Komrower J, Lau J. Experimental modal analysis: efficient geometry model creation using optical techniques. Journal of the IEST 2006;49(2):104–13.
[20] Armesto J, Lubowiecka I, Ordóñez C, Rial FI. FEM modeling of structures based on close range digital photogrammetry. Automation in Construction 2009;18(5):559–69.
[21] Meyer CG, Jones TW, Lunsford CB, Pappa RS. In-vacuum photogrammetry of a 10-meter solar sail. In: collection of technical papers - AIAA/ASME/ASCE/AHS/ASC structures, structural dynamics and materials conference 2; 2005. p. 1004–1015 AIAA-2005-1889.
[22] Schmidt T, Tyson J, Galanulis K. Full-field dynamic displacement and strain measurement using advanced 3D image correlation photogrammetry: part I. Experimental Techniques 2003;27(3):47–50.
[23] Schmidt T, Tyson J, Galanulis K. Full-field dynamic displacement and strain measurement - specific examples using advanced 3D image correlation photogrammetry: part II. Experimental Techniques 2003;27(4):22–6.
[24] Schmidt T, Tyson J, Galanulis K, Revilock D, Melis M. Full-field dynamic deformation and strain measurements using high-speed digital cameras. proceedings of SPIE - The International Society for Optical Engineering; 2005.
[25] Haritos N, Hira A, Mendis P, Perera U. Repair and strengthening of reinforced concrete structures using CFRPs. Advances in Structural Engineering 2006;9(1):1–9.
[26] Pappa RS, Lassiter JO, Ross BP. Structural dynamics experimental activities in ultralightweight and inflatable space structures. Journal of Spacecraft and Rockets 2003;40(1):15–23.
[27] Grytten F, Fagerholt E, Auestad T, Førre B, Børvik T. Out-of-plane deformation measurements of an aluminium plate during quasi-static perforation using structured light and close-range photogrammetry. International Journal of Solids and Structures 2007;44(17):5752–73.
[28] Chang CC, Ji YF. Flexible videogrammetric technique for three-dimensional structural vibration measurement. ASCE Journal of Engineering Mechanics 2007;133(6):656–64.
[29] Chang CC. From photogrammetry, computer vision to structural response measurement. Proceedings of SPIE - the international society for optical engineering; 2007. 652903.
[30] Simpson A, Smith SW, Jacob J. Aeroelastic behavior of inflatable wings: wind tunnel and flight testing. In: collection of technical papers - 45th AIAA aerospace sciences meeting; 2007.
[31] Ji Y, Chang CC. Identification of structural dynamic behavior for continuous system based on videogrammetric technique. Proceedings of SPIE - The International Society for Optical Engineering; 2006. 61731I.
[32] Black JT, Pappa RS. Photogrammetry and videogrammetry methods for solar sails and other gossamer structures. In: collection of technical papers - AIAA/ASME/ASCE/AHS/ASC structures, structural dynamics and materials conference; 2004.
[33] Pappa RS, Black JT, Blandino JR, Jones TW, Danehy PM, Dorrington AA. Dot-projection photogrammetry and videogrammetry of Gossamer space structures. Journal of Spacecraft and Rockets 2003;40(6):858–67.
[34] Helfrick M, Niezrecki C, Avitabile P, Schmidt T. 3D digital image correlation methods for full field vibration measurement. In: the 26th IMAC, International Modal Analysis Conference Proceedings. Orlando, Florida; 2008.
[35] Helfrick M, Niezrecki C, Avitabile P. Optical non-contacting vibration measurement of rotating turbine blades. In: the 27th IMAC, International Modal Analysis Conference Proceedings. Orlando, Florida; 2009.
[36] Warren C, Niezrecki C, Avitabile P. Applications of digital image correlation and dynamic photogrammetry for rotating and non-rotating structures. In: the 7th international workshop on structural health monitoring. Stanford, CA; 2009.
[37] Corten GP. Optical motion analysis of wind turbines. In: European Union wind energy conference. Bedford UK; 1996.
[38] Website 1. Nordex wind energy, http://www.nordex-online.com/en/products-services/wind-turbines/n80-25-mw/ [accessed April 2010].
[39] Website 2. GOM optical measuring techniques, http://www.gom.com [accessed April 2010].
[40] Website 3. ECN energy research center of the Netherlands, http://www.ecn.nl/units/wind/wind-turbine-testing/ [accessed April 2010].
[41] Murtagh PJ, Basu B, Broderick BM. Mode acceleration approach for rotating wind turbine blades. Proceedings of the Institution of Mechanical Engineers. Part K: Multi-body Dynamics 2004;218:159–67.
[42] Murtagh PJ, Basu B, Broderick BM. Along-wind response of a wind turbine tower with blade coupling subjected to rotationally sampled wind loading. Engineering Structures 2005;27:1209–19.
[43] Ozbek M, Meng F, Rixen DJ, van Tooren MJL. Identification of the dynamics of large wind turbines by using photogrammetry. In: the 28th IMAC, International Modal Analysis Conference Proceedings. Jacksonville, Florida; 2010.